Semiconductor Physics, Quantum Electronics & Optoelectronics. 2003. V. 6, N 4. P. 479-486.

PACS: 68.65.Fg

Structural changes in multilayer systems containing $In_xGa_{1-x}As_{1-y}N_y$ quantum wells

I.M. Fodchuk, V.B. Gevyk, O.G. Gimchinsky, E.N. Kislovskii*, O.P. Kroytor, V.B. Molodkin*, S.I. Olihovskii*, E.M. Pavelescu, M. Pessa****

Yu. Fedkovich Chernivtsi national university, Chernivtsi
**G.V. Kurdyumov Institute for Metal Physics, NAS of the Ukraine, Kyiv*
*** Optoelectronics Research Centre, Tampere university of Technology, Tampere, Finland*

Abstract. The investigations of multilayer nano-scale systems contained one or two quantum wells are carried out by double-crystal X-ray diffractometry. Processes of interdiffusion of In, Ga atoms and their influence on properties of such systems are considered. The content of nitrogen in quantum wells and buffer layers are defined. It is determined that $In_xGa_{1-x}As_{1-y}N_y$ system has perfect crystalline structure, and interface between layers is coherent.

Keywords: lattice matching, rocking curves, interdiffusion, superlattices.

Paper received 19.09.03; accepted for publication 11.12.03.

1. Introduction

Multilayer semiconductor $A^{III}B^{IV}$ compounds are perspective for the development of the next generation of solar cells with expected efficiency higher than ~40 %. The quaternary system $In_xGa_{1-x}As_{1-y}N_y/GaAs$ is the most suitable for such devices [1]. It is known [1–7], that adding In atoms in GaAs increases both lattice constant a and band gap E_g, while incorporation atoms of nitrogen (N) into GaAs decreases both a and E_g. By doping In and N in GaAs we can simulate areas of necessary band gaps and lattice constant with the purpose of obtaining desirable photovoltaic properties. For example, system $In_xGa_{1-x}As_{1-y}N_y$ can be lattice matched to GaAs with $E_g \cong 1$ eV, at the $x = 3y$ and $y \approx 3\%$. However, preparation of $In_xGa_{1-x}As_{1-y}N_y/GaAs$ compounds with desired good quality has still some technical problems at present time. The crystal quality deteriorates rapidly with increasing N content, because the local strain and clustering in layers increases [4–8].

The most available tool for structural diagnostics of semiconductor nano-scale multilayer compounds is the X-ray double-crystal diffractometry [9]. On its basis the high-efficiency experimental and theoretical researches of interdiffusion processes and strain relaxations in ultra thin epitaxial layers of layered structures is performed [9,10].

The main purpose of this work was to is investigate interdiffusion processes of In and Ga atoms in multilayer systems on GaAs substrate which contain $In_xGa_{1-x}As_{1-y}N_y$ quantum wells (QW) using the high-resolution X-ray double-crystal diffractometry.

2. Theoretical basis

For structures with one layer the typical parameters as lattice mismatch, chemical composition and layer thickness can be easy determined by non-destructive X-ray methods [8,9,11,12]. However for multilayer systems the interference of X-rays scattered by different layers, results in the complex diffraction curves that cannot be unambiguously interpreted by traditional techniques.

Now kinematical and dynamical theories is used for simulation of X-ray diffraction processes in multilayer nano-scale systems. In the kinematical theory the multiple scattering is neglected calculating the Bragg rocking curves for layers with a thickness less then that of extinction. The dynamical scattering theory takes into account these effects, and thus it is not limited by the thickness of a crystal layer. It is efficiently used for the analysis of rocking curves (RCs) from heterostructures with matched or closed matched lattices [12,13].

According to Takagi-Taupin theory, the differential equation for amplitude relation $D_{0,h}/D_a$ of scattered $D_{0,h}$ and incident D_a waves can be given by [8,12]:

$$i\frac{dX}{dA} = (1+ik)X^2 - 2(y+ig)X + (1+ik), \quad (1)$$

where $X = D_h/(\beta^{1/2}D_0)$, D_0, D_h are the scattering amplitudes of transient and diffracted waves, respectively, $\beta = |\gamma_0/\gamma_h|$, $A = (P\pi \mid \chi'_h \mid z)/\lambda \mid \gamma_0\gamma_h \mid^{1/2}$, λ is the X-ray wavelength, z is the layer thickness, P is the polarization coefficient, $g = (1+\beta)\chi''_0/(2P \mid \chi'_h \mid \beta^{1/2})$, $k = \chi''_h/\chi'_h$. γ_0, γ_h are cosines of incident and reflection angle accordingly, $y = [(1+\beta)\chi'_0 - \beta\alpha_h]/(2P \mid \chi'_h \mid \beta^{1/2})$, $\alpha_h = -2\Delta\theta \times \sin 2\theta_B - \alpha_s$, $\alpha_s = C\varepsilon(z)$, $\Delta\theta$ is the angular deviation of incident beam from the Bragg angle θ_B, $\varepsilon(z)$ is the one-dimensional strain, $C = \cos^2\varphi\,\mathrm{tg}\theta_B \pm \sin\varphi\cos\varphi$, where + is corresponded to grazing incident angle ($\theta_B - \varphi$) concerning the sample surface, – to the ($\theta_B + \varphi$) angles; φ is the angle between reflecting plane and the sample surface, χ_0, χ_h are the Fourier coefficients of the crystal polarizability.

Rocking curves represent the dependence of X-rays reflectivity R on $\Delta\theta$, $R = X(\Delta\theta)X^*(\Delta\theta)$ (* signifies complex conjugation).

At present, the numerical integration of the equation (1) is carried out by the Runge-Kutt method of the fourth and fifth orders. Less rigorous methods used for near kinematical approximations [2,14,15] are also known.

The basic difficulty of numerical solution (1) is ambiguity of definition of S parameter at different values $\Delta\theta$ and ε. The scattering amplitude should approach to zero at $\Delta\theta \to \infty$, and dependence $X(\Delta\theta)$ – to be the continuous [13]. Ordinate of each point of RC is function of all strain profile $\varepsilon(z)$ determined by solution of inverse problem of X-ray diffraction on known RC. In this method minimization of nonnegative discrepancy between the experimental and theoretical RCs is used [3,14–16]. To increase the contribution of side regions and satellite maxima of RC, we used the functional in the following form

$$\Phi = \sum_n g(\theta_n)(R_n^{theory} - R_n^{\exp})^2, \quad (2)$$

where $g(\theta_n) = 1 - (1 + (\theta_n - \theta_0)^2 W)^{-1}$ is the weighted function, θ_n is the abscissa of n-th point on RC, θ_0 is the abscissa of the basic maximum corresponded to scattering from substrate, W is the inverse value of RC half-width for ideal crystal.

3. Investigation object

Investigated samples were grown on GaAs (001) substrates by molecular-beam epitaxy (MBE) in Optoelectronics Research Center of Tampere Technology University (Finland). Layers thickness was defined by reflectivity oscillations of high-energy electron diffraction.

Firstly nitrogen concentration in layer was evaluated by angular misorientation between reflection maxima from substrate and from relevant layers. Then it was defined more precisely by fitting the calculated RCs to experimental.

Measurements of RCs were carried out by double-crystal X-ray diffractometer "Bede" with copper tube (λ = 0.15405 nm). The collimated monochromatic X-ray beam was formed by using symmetrical monochromator GaAs (001) in (004) reflection. The reflected beam was detected by the scintillation counter with a narrow slit during the $\theta - 2\theta$ scanning nearby the symmetric (004) reflection over 16 hours.

In many researches shown were [15] that the most of N atoms occupies sites of As sublattice. It is noted that appearance of isolated interstitial N in GaNAs is energetically unprofitable. Formation of As-N or N-N complexes is possible in interstitial positions of lattice, but first is more energy advantageous [17]. N-As complexes caused compressive strains in the epilayer whereas N-N complexes constricted it in comparison with substitutional atom N_{As}. Interlinking these unsubstituted N atoms results in deviation from Vegard's law [17] and additional angular misorientation of RC.

To simulate X-ray RCs by using Takagi-Taupin formalism, the strains caused by lattices mismatch between thin QW and thick barrier layer have been taken into account. In our case, QW is pseudomorphous and lattice constant is uniform throughout the whole structure [18]. The mismatch creates tetragonal deformation in the lattice and manifests as the strain perpendicular to the heterointerface. If the growth direction Oz is along <001>, the GaInNAs well layer is subjected to biaxial compression in-plane strains parallel to the Ox direction along <100> and Oy direction along <010>. The biaxial in-plane strains and uniaxial shear strains after interdiffusion are given by

$$\varepsilon_{xx} = \varepsilon_{yy} = \varepsilon_{\mathrm{mis}}(x), \quad (3a)$$

$$\varepsilon_{zz} = -2[c_{12}(x)/c_{11}(x)]\varepsilon_{\mathrm{mis}}(x), \quad (3b)$$

where $\varepsilon_{\mathrm{mis}}(x)$ is the mismatch factor between well and the barrier which is negative for compression strains, $c_{12}(x)$ and $c_{11}(x)$ are the elastic stiffness constants. The generalized parameter a for quaternary compounds $A_xB_{1-x}C_yD_{1-y}$ [19] is defined from parameters of four binary compounds AB, AD, BC, CD:

$$a(x, y) = (1 - x)ya\mathrm{BC} + xya\mathrm{AC} + x(1 - y)a_{\mathrm{AD}} + (1 - x)(1 - y)a_{\mathrm{BD}}. \quad (3c)$$

If $x, y << 1$ the Eq. (3c) shows, that a parameter of layer almost linearly depends on values of y and x. Apparently, the same dependence should be observed for mismatch between lattice parameters of layer and substrate.

However, strains around quantum dots [20] and in layers interfaces are too complicated for description within the framework of simple analytical expressions (3a,b). The average strain value can be estimated via:

$$\varepsilon_{\parallel}^{L} = \frac{a_{\parallel}^{L} - a_0^S}{a_0^S}, \quad \varepsilon_{\perp}^{L} = \frac{a_{\perp}^{L} - a_0^S}{a_0^S}, \tag{4}$$

where index L is referred to heteroepitaxial layer, S – to substrate, $\perp$ – to growth direction and 0 – to case of strain absence. For the thin coherently growth film on thick substrate $a_{\parallel}^{L} = a_0^S$, then $\varepsilon_{\parallel}^{L} = 0$ and $a_{\perp}^{L}$ is calculated as

$$a_{\perp}^{L} = \frac{c_{11} + 2c_{12}}{c_{11}}\left(a_0^L - a_0^S\right) + a_0^S . \tag{5}$$

According to X-ray topography, misfit dislocations in studied samples were rarely observed. The critical strain magnitude of misfit dislocation formation ε_{cr}^{MD} is estimated by [14]

$$\varepsilon_{cr}^{MD} = \frac{b}{8\pi(1-\nu)h}\left(\frac{1-2\nu}{1-\nu}\right)\left(\ln\frac{2h}{b} - \frac{1}{2}\right), \tag{6}$$

and its value is equal $\varepsilon_{cr}^{MD} = 6.17 \cdot 10^{-3}$ at the layer thickness $h = 6.8$ nm, the Burgers vector $b = 0.4$ nm ($b = a/2\langle 110\rangle$), Poisson's ratio $\nu = 0.352$. Obviously, for most of the samples $\varepsilon_{cr}^{DM} > \varepsilon_{mis}$.

4. Results

Interdiffusion is a thermal process that assists the movement of atoms near heterointerface. Such movement will changes both band structure and properties of QW [1–7, 19]. It is shown that short-time annealing of GaInNAs improves photoluminescent and other photoelectric properties, but the complete explanation of this phenomenon not exists yet [21]. Complex investigations of influence of technology factors on degree of material structural perfection can give understanding of structural changes at annealing and its correlations with electronic properties [5,6,22].

During annealing, the following structural modifications can happen. Nitrogen, linked with In atom, relaxed in a direction to the Ga atoms, reducing strain and increasing frequency Ga-N bond in NGa_3In cluster regard to Ga_4N cluster. It explains displacement of photoluminescent maximum in "blue" spectral range [19]. After growth nitrogen atoms are situated in lattice sites and surrounded by four atoms of gallium. At annealing, the local strain is decreased by formation of In-N bonds. It caused probably by nitrogen transition, but the possibility of indium movement is not excluded. Except formation of In-N pairs, another structural modification, namely formation of new Ga-N bands also takes place. After annealing most of the nitrogen atoms are located in NGa_3In clusters. Formation of this cluster that contains In-N band reduces strains in the system [16].

4.1. Multilayer structure with QW of $In_xGa_{1-x}As$ type

The scheme of multilayer structure with such QW is shown on insert of Fig. 1. Well width is 6.8 nm (12 atomic layers), $x = 0.37$. Layer thickness is less than critical thickness necessary for the formation of misfit dislocations. The experimental and calculated RCs of multilayer system are shown in Fig. 1.

The maximum of QW reflection intensity on the experimental RCs (Fig. 1a) is displaced from the main maximum (corresponding to GaAs substrate) on $\Delta\theta_{QW} = 5920 \pm 10$ arc.sec. Some magnification of $\Delta\theta_{QW}$, (~ on 50 arc.sec) is observed for annealed structure in comparison with unannealed one. The interface becomes more roughened due to interlayer interdiffusion In↔Ga or the relaxation of elastic strains between layers or appearance of quantum dots and dislocations.

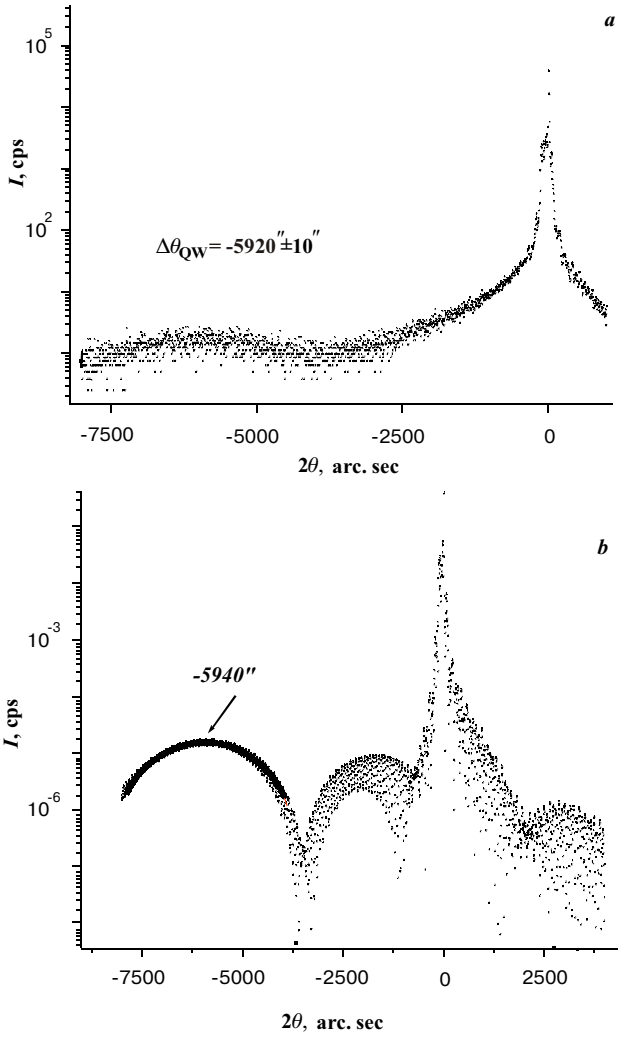

Fig. 1. Experimental (a) and calculated (b) RCs for multilayer system with $In_{0.37}Ga_{0.63}As$ QW.

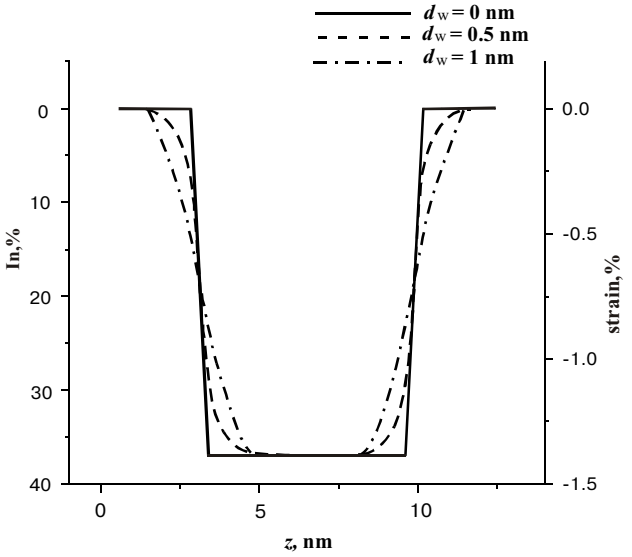

Fig. 2. Scheme of distribution of misfit strains due to redistribution In in and outside of QW at smearing. Width of QW is 6.8 nm (12 monolayers $In_{0,37}Ga_{0,63}As$), at $d_w = 0$ nm QW is not smeared, at $d_w = 0.5$ nm we have 1-st variant of smearing, $d_w = 1.2$ nm – 2-nd variant.

From carried out researches follows, that the quantitative and qualitative agreement between calculated and experimental RCs is possible taking into account the QW smearing (Fig. 2) only. Local disorder in spaces between neighbour heterolayers can cause various microstructural fluctuations in $In_xGa_{1-x}As_{1-y}N_y$ films. Due to this, interfaces between thin $In_xGa_{1-x}As_{1-y}N_y$ layers and GaAs have smear shape, with average interphase roughness within the range 5–20Å [7,18]. Fig. 1b shows RC calculated taking into the consideration process of interlayer interdiffusion in QW. Increasing x by 0.01 increases angular misorientation between maxima from QW and substrate by 180 arc.sec. The best coincidence of calculated and experimental RCs is observed at 2-nd variant of QW smearing (Fig. 2).

As locations of QW reflection maxima before and after annealing had changed insignificantly, we shall assume that main process of QW smearing have happened during growth yet. It should be noted that considerable In-Ga intermixing on interface happened even in as-growth QW of $In_xGa_{1-x}As$/GaAs type [18]. By interdiffusion of elements of III-group during QW growth, In atoms diffused to barrier GaAs layer, and Ga atoms to QW [19]. The results of research shown that the thin and graded interface was generated with thickness $2d_w$ (Fig. 2). For as-growth $In_xGa_{1-x}As$/GaAs sample, the best agreement between the experimental and simulated RCs is achieved at QW smearing on depth of 1.2 nm (two atomic layers at both sides of QW center) and general decreasing In content on 19 %. During fast thermal annealing the ordering of In-Ga atoms can happen in produced interlayer region that also caused reduction of strains in structure.

Efficient thickness d_w of layers smearing (it can be compared to the length of In-Ga interdiffusion) also can increase at increasing the substrate temperature. Accordingly, thickness d of $In_xGa_{1-x}As_{1-y}N_y$ layers decreases. However, $d_w + d$ does not changes during heightening process of the following layers [20].

The possible variants of QW smearing (Fig. 2) are taken into account at calculation of RC for the given multilayer structure. Various concentrations of nitrogen in QW and buffer layers as well as their influence on shaping of RC structure were considered. The distribution of In and Ga atoms in QW (Fig. 2) is described by distribution function [23]

$$x(z) = \frac{x_0}{2}\left[\mathrm{erf}\left(\frac{L_z + 2z}{4d_w}\right) + \mathrm{erf}\left(\frac{L_z - 2z}{4d_w}\right)\right], \qquad (7)$$

where L_z is the QW width, x_0 is the In content in QW, z is the coordinate, $z = 0$ corresponds to QW center. As and N concentration profiles do not vary. Ga concentration does not change in central region of QW, and the diffusion length increases from 0 to 1.1 nm (Fig. 2).

From the analysis of the experimental RCs, the diffusion of In atoms in the barrier layer reduces lattices mismatch in the heterojunction. It causes strain relaxation in layers near QW. For as-grown layer with QW the misfit deformation is 1.3 % at center of QW. Interdiffusion reduces a compressive strain up to 0.98 % on interface between layer and QW. In barrier area the compressive strains increase, because In content increases near the surface. Compressive strains achieve 0.25 % at the diffusion length $L_d = 0.565$ nm.

4.2. Multilayer structure with QW of $In_xGa_{1-x}As_{1-y}N_y$ type

The investigation results of series of samples with various QW width and N contents are considered in this part. According to technological conditions it is known that $x = 0.37$. The special experimental RCs for some sample are shown in Fig. 3.

Presence of nitrogen in QW reduces angular misorientation $\Delta\theta_{QW}$ and lattice mismatch parameters correspondingly [18]. Angular misorientation between layer and substrate decreases by 500 arc.sec at N concentration increasing by 1%. The analysis of calculated RCs without smearing and with smearing of QW (Fig. 2) enables to estimate N content in QW with accuracy of 0.05 %.

The dynamical theory of X-ray scattering was used for the more complete agreement between theoretical and the experimental RCs. The best coincidence of these RCs was obtained by taking into account instrumental factors as well as parameters of atomic roughness of interlayer interfaces.

In comparison with InGaAs QW (Fig. 1), the angular misorientation between InGaAsN QW and substrate maxima strongly decreases by 1070 arc.sec (Fig. 3).

As in the previous case, distribution of In and Ga atoms in QW is described by Eq. (7) because the concentra-

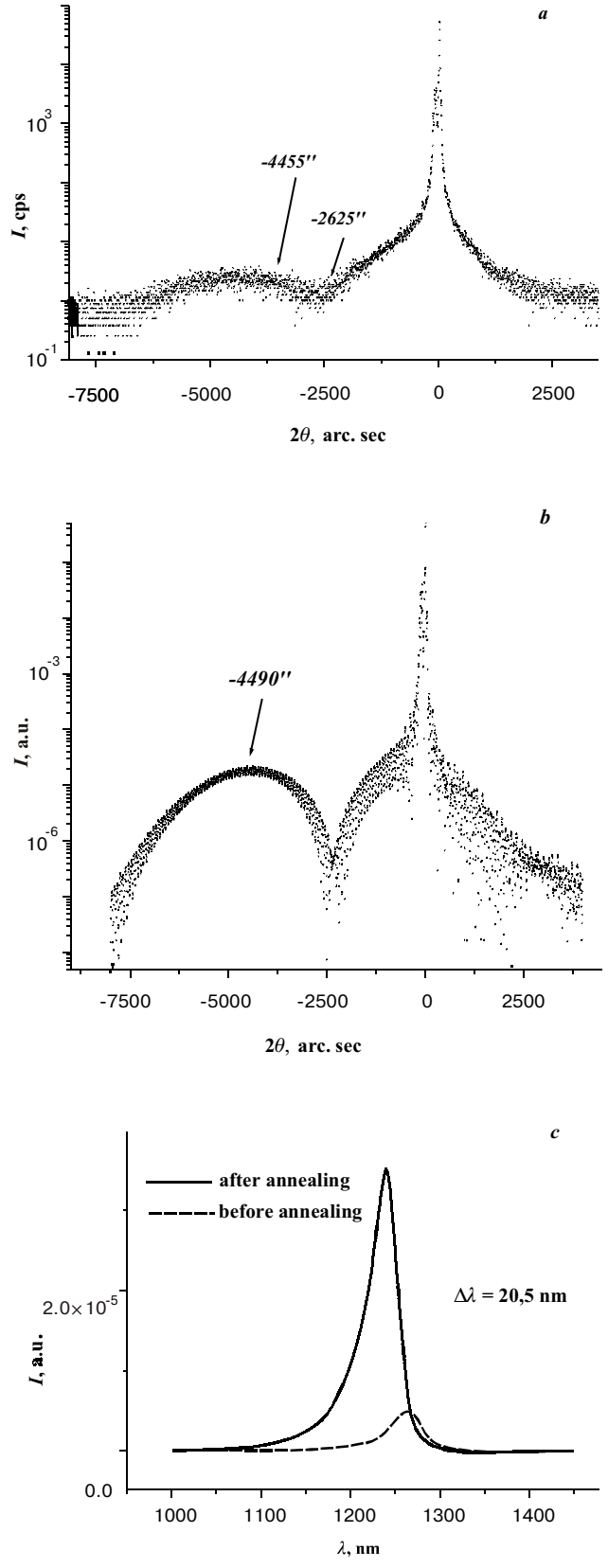

Fig. 3. Experimental (a) and calculated (2-nd variant of smearing) (b) RCs from multilayer system with $In_{0.37}Ga_{0.63}As_{1-y}N_y$ QW, $y \cong 3.1\%$; PL spectrum (c).

tion profile of As and N does not change. Ga atoms near interface diffuse to QWs, and In atoms – to the barrier. Ga concentration in central region of QW does not vary, and the diffusion length increases from 0 to 1.1 nm.

From the analysis of the experimental RCs, it follows that the diffusion of In atoms in the barrier layer reduces lattice mismatch in the heterojunction, and causes strain relaxation in the next QW layers. For as-grown QW layer the mismatch strain is equal to 1.3 % at the center of QW. Interdiffusion reduces the compressive strain up to 0.98 % on the interfaces with QW. In the barrier layer, compression strains increase, since concentration of In atoms near the surface increase. At the diffusion length L_d = 0.565 nm the compression strains are equal to 0.25 %.

For annealed samples, some reduction of angular misorientation of QW in comparison with unannealed samples is observed. A reason of it can be strain reduction on interfaces between layers owing to interlinking atoms In by atoms N.

Theoretical simulation of RCs for various N concentrations in QW have shown that y increasing on 1 % have reduced angular misorientation between QW and GaAs substrate by 505 arc.sec. independently of the smearing degree of QW. At increase of the nitrogen concentration, the first intensity oscillations on both sides of the main maximum disappear, and QW reflection has more expressed asymmetric shape.

Let's mark, that after short-time annealing (~10 sec) of the given system the location of reflection maximum for substrate was not almost varied. For annealed samples the slight decreasing of angular misorientation (by 30–40 arc.sec) of layer with respect to substrate is observed in comparison with unannealed samples.

4.3. Multilayer structure with buffer $GaAs_{1-y}N_y$ layers and QW of $In_xGa_{1-x}As_{1-y}N_y$ type

Difference of the given structure and previous one consists in amount of subsidiary layers and presence of buffer $GaAs_{1-y}N_y$ layers on each side of QW (see insertion in Fig. 4).

To improve GaInNAs/GaAs quality N content in QW was reduced, though it caused increasing of strains in quantum wells. Due to compensating barrier in that system GaInNAs QWs is characterized by high structural perfection, without mismatch strains [22]. It enables to increase the number of QWs in a laser structure (Fig. 5).

Let's consider a new system with GaInNAs QW, which contains the strain-compensating barrier GaAs layers grown by MBE from gas origin. A series of samples with different temperature conditions of QW formation are studied. QW width for most of the samples was 6.8 nm (12 atomic layers).

The typical experimental RCs before and after annealing of multilayer system are shown in Fig. 4. RCs for other samples have the same shapes and differed only by displacements of intensity maxima from QWs and buffer layers.

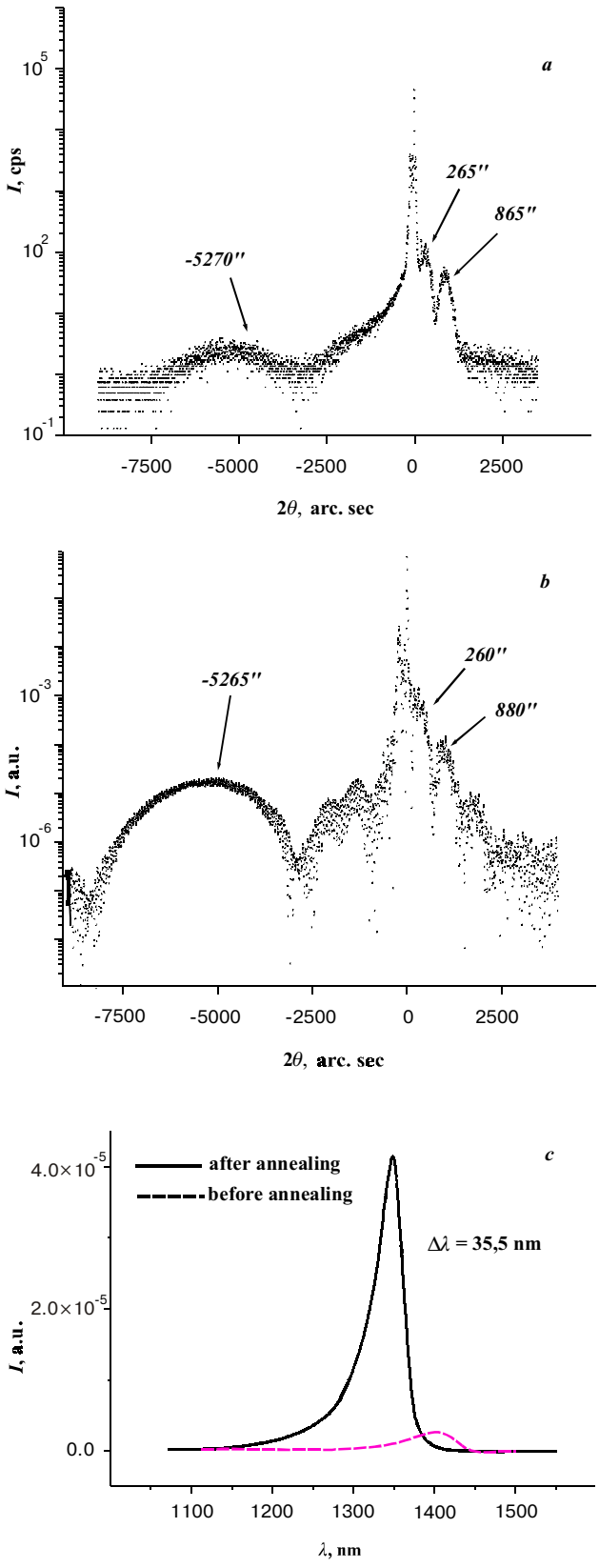

Fig. 4. Experimental (a) and calculated (b), RCs for system of $In_{0.37}Ga_{0.63}As_{1-y}N_y$ QW with $GaAs_{1-y}N_y$ buffer layers, $x = 0.37$ (In), $d = 6.8$ nm (12 monolayers), $\theta - 2\theta$ scanning step is 5 arc.sec. PL spectrum before and after annealing (c). N content in QW and buffer layers is 2,1 % and 1 % respectively.

In contrast to the previous case of multilayer structure, the system of intensity maxima are observed on the experimental RCs. They are caused by reflections from GaAs substrate, from $GaAs_{1-y}N_y$ buffer layers at right side of RC corresponding to the main peak, and from QW at left-hand part of RC. Besides, the fine oscillation structure is observed on peaks from buffer layers, which indicates high coherence of layers. For the given structure above-mentioned variants of possible QW smearing (Fig. 2) are used when analyzing the experimental RCs. Different variants of nitrogen contents in QW and buffer layers, as well as their influence on formation of RC structure are considered.

Obviously, luminescent intensity for the structure with compensated strain is higher than for structure with GaAs barrier. It indicates better quality of material (Fig. 4). Photoluminescent (PL) maxima from as-grown GaInNAs/GaAs quantum well are insignificant due to defects linked with N and damages caused by N ions in GaInNAs layer. At smaller temperatures, a lot of point defects penetrates in GaInNAs due to decreasing of cations migration. To improve quality of material, the annealing of samples were carried out at different temperatures and time. For GaInNAs/GaAs structures the intensity of PL was considerably increased. In Fig. 4c PL intensity increased with increasing of annealing temperature up to 650°C over 10 s and then reduced. At increasing of speed of thermal annealing PL-peaks were displaced in "blue" region for all QWs, that probably, predetermined by diffusion of In, Ga, N.

The analysis of calculated RCs without and with taking into account QW smearing, enables to estimate concentration of nitrogen in buffer layers and in QW. Considerable decreasing of $\Delta\theta_{QW}$ is observed in contrast to the system without nitrogen.

4.4. Multilayer system with two $In_{0.37}Ga_{0.63}As_{1-x}N_x$ quantum wells

Let's consider a new multilayer system with two GaInNAs QW, which contains the strain-compensating GaAs barrier layers grown by MBE from gas origin (insertion in Fig. 5).

Heteroboundary morphology plays an active role in forming of physical properties in this multilayer structure. Thus inspite of the fact that addition of N in InGaAs reduces a lattice mismatch between InGaAs and GaAs, the so-called 3D-growth (island-like) of InGaAsN layer is possible [4].

The well-defined oscillation structure of intensity in the experimental RCs (Fig. 5) at left-hand of QW indicates high coherence and perfection of this multilayer system. In contrast to the previous case of multilayer structure in the experimental RCs, the whole system of intensity maxima, caused by consecutive reflections of X-rays from QW (intensity oscillations system is the interference interaction of diffracted waves from two QWs), from GaAs substrate at the center, and from buffer layers $GaAs_{1-y}N_y$ in right-hand of RC are observed. The fine

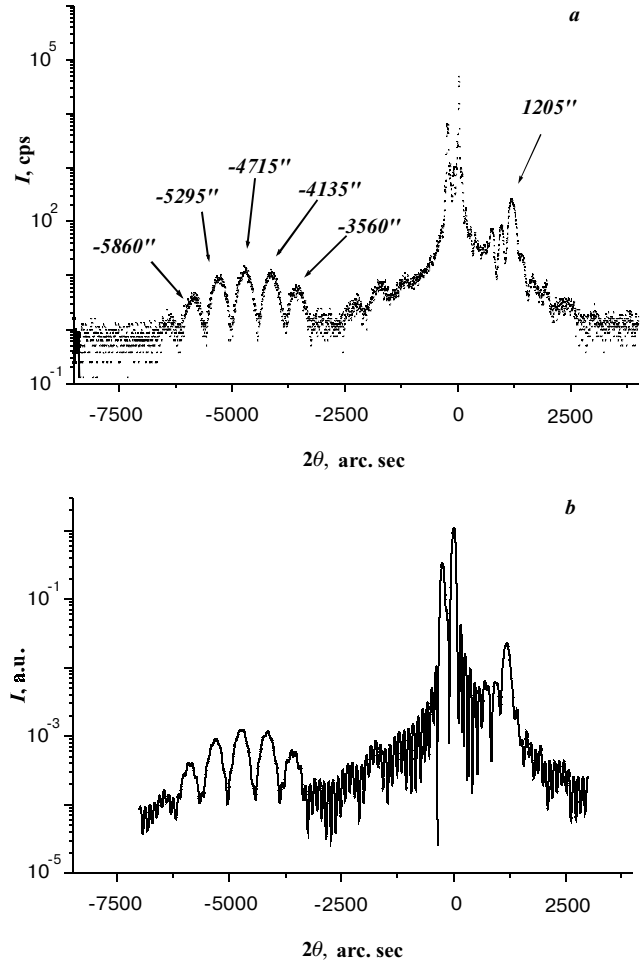

Fig. 5. Multilayer system contained two $In_{0.37}Ga_{0.63}As_{1-y}N_y$ quantum wells $d = 6.8$ nm. Experimental (a) and calculated (b) RCs. $y = 2.4$ % in QW and 1 % in buffer layers.

oscillation structure of reflection from QW indicates high coherence of these layers.

The interface of given structure as result of interdiffusion of atoms, changes from sharp to smearing profile (Fig. 2) as it was supposed in previous cases. For satisfactory agreement of theoretical and the experimental RCs all possible variants of QW smearing are taken into account. The best quantitative and qualitative correspondence between calculated and the experimental RCs takes place at $y = 2.4$ % (N) in both QWs and $y = 1$ % in buffer layers.

For the complete agreement of calculated and the experimental RCs, it should be taking into account nonlinearity of relaxation of elastic strains between layers, appearance of quantum dots and dislocations that result to considerable roughness of interface [18].

5. Conclusions

The double X-ray diffractometry is the efficient non-destructive tool to examination of ultrathin heterophase multilayer systems.

1. The multilayer semiconductor systems containing quantum wells were investigated by high-resolution X-ray diffractometry. The degree of interlayer interdiffusion before and after annealing was defined by fitting the calculated and experimental RCs.

Changes of nitrogen content in QW are determined in dependence on growth conditions.

2. In as-grown multilayer structures with QW, the processes of interdiffusion revealed by smearing of QW, i.e. diffusion In to buffer or cap layers and Ga to QW take place. Short-time temperature annealing slowly reduces angular misorientation between QW and substrate.

3. Experimentally obtained and theoretically designed RCs indicates the perfection of crystalline structure of multilayer structure on GaAs substrate and coherence of interfaces between cap, buffer layers and QW in system of $GaAs/GaN_xAs_{1-x}/In_xGa_{1-x}As_{1-y}N_y/GaN_xAs_{1-x}/GaAs$ type.

4. The nitrogen content in QW and buffer layers depends on various technology factors, for example, temperature of substrate. Thus, the arbitrary distribution of In and N impurities in such systems can determine either increasing or reducing of degree of local disordering and strains.

References

1. I. Vurgaftman, J.R. Meyer, L.R. Ram-Mohan, Band parameters for III–IV compound semiconductors and their alloys // *Journal of Applied Physics*, **89**(11), pp. 5815-5875 (2001).
2. C.E. Zah, R. Bhat, B.N. Pathak, F. Favire, W. Lin, M.C. Wang, N.C. Andreadakis, D.M. Hwang, M.A. Koza, T.P. Lee, Z. Wang, D. Darby, D. Flanders, J.J. Heieh, High-performance uncooled 1.3 μm $Al_xGa_yIn_{1-x-y}$ As/InP strained-layer quantum-well lasers for subscriber loop applications // *Journal of Quantum Electronic*, **30**, pp. 511-523 (1994).
3. D.E. Mars, D.I. Babic, Y. Kaneko, Y.-L. Chang, Growth of 1.3 μm InGaAsN laser material on GaAs by molecular beam epitaxy // Journal of Vacuum Science and Technology, **17B**, pp. 1272-1275 (1999).
4. J.C. Harmand, G. Ungaro, L. Largeau, G.TLe Roux, Comparison of nitrogen incorporation in molecular-beam epitaxy of GaAsN, GaInAsN, GaAsSbN // *Applied Physics Letters*, **77**(16), pp. 2482-2484 (2000).
5. A. Al-Yacoub, L. Bellaiche, Quantum mechanical effects in (Ga,In)(As,N) alloys // *Physical Review*, **62B**(16), pp. 10847-10851 (2000).
6. E.D. Lones, N.A. Modine, A.A. Allerman, S.R. Kurtz, A.F. Wright, S.T. Tozer, X. Wei, Band structure of $In_xGa_{1-x}As_{1-y}N_y$ alloys and effects of pressure // *Physical Review*, **60B**(No.7), pp. 4430-4433 (1999).
7. Y.L. Soo, S. Huang, Y.H. Kao, J.N. Chen, S.L. Hulbert, J.F. Geisz, S. Kurtz, J.M. Olson, S.R. Kurtz, E.D. Jones, A.A. Allerman, Local structures and interface morphology of $In_xGa_{1-x}As_{1-y}N_y$ thin films grown on GaAs // *Physical Review*, **60B**(19), pp. 13605-13611 (1999).

8. P.F. Fewster, Alignment of double-crystal diffractometers // Journal of Applied Crystallography, **18**, pp. 334-338 (1985).
9. X. Chut, B.K. Tanner, Double crystal x-ray rocking curves of multiple layer structures // *Semicond. Sci. Technol*, **2**, pp. 765-771 (1987).
10. M. Kondow, T. Kitatani, K. Nakahara, T. Tanaka, Temperature dependence of lasing wavelength in a GaInNAs laser diode // *IEEE Photonics Technol. Lett*, **12**, pp. 777-779 (2000).
11. P.F. Fewster, X-ray diffraction tools and methods for semiconductor analisis // *Inst. Phys. Conf*, **164**, pp. 197-206 (1999).
12. P.F. Fewster, C.J. Curling, Compositional lattice-mismatch measurement of thin semiconductor layers by x-ray diffraction // *J. Appl. Phys*, **62**, pp. 4154-4158 (1987).
13. S.A. Takagi, Dynamical theory of difraction for a distorted crystal // *J. Phys. Soc. Japan*, **26**(5), pp. 1239-1253 (1969).
14. Wei Li, M. Pessa, T. Ahlgren, J. Decker, Origin of improved luminescence efficiency after annealing of Ga(In)NAs materials grown by molecular-beam epitaxy // *Applied Physics Letters*, **79**(8), pp. 1094-1096 (2001).
15. T. Anan, K. Nishi, K. Sugou, M. Yamada, K. Tokutoe, A. Gomyo, GaAsSb: A novel material for 1.3 μm VCSELs // *Electron. Lett*, **34**(22), pp. 2127-2129 (1998).
16. F. Hoehnsdorf, J. Koch, S. Leu, W. Stolz, B. Borchert, M. Druminsk, Reduced threshold current densities of (Galn)(NAs)/GaAs single quantum well lasers for emission wavelengths in the range 1.28–1.38 μm // *Electron. Lett*, **35**(7), pp. 571 (1999).
17. Wei Li, M. Pessa, L. Likonen, Lattice parameter in GaNAs epilayers on GaAs: Deviation from Vegard's law // *Applied Physics Letters*, **78**(19), pp. 2864-2866 (2001).
18. V.B. Molodkin, M. Pessa, E.M. Pavelesku, I.M. Fodchuk, E.N. Kislovsky, S.I. Olichovsky, T.P. Vladimirova, O.G. Gimchynsky, O.P. Kroytor, E.S. Skakunova, X-Ray diffraction investigations of $In_xGa_{1-x}As_{1-y}N_y$/GaAs Multilayered Structure // *Metalofizika i novitni tehnologii*, **24**(4), pp. 477-495 (2002).
19. M.C.Y. Chan, C. Surya, P.K.A. Wai, The effects of interdiffusion on the subbands in $In_xGa_{1-x}As_{0.96}N_{0.04}$/GaAs quantum well for 1.3 and 1.55 μm operation wavelengths // *Journal of Applied Physics*, **90**(1), pp. 197-201 (2001).
20. S.J. Xu, H. Wang, Q. Li, M.H. Xie, X.C. Wang, W.J. Fan, S.L. Feng, X-ray diffraction and optical characterization of inter diffusion in self-assembled InAs/GaAs quantum-dot superlattices // *Physics Letters*, **77**(14), pp. 2130-2132 (2000).
21. W. Li, J. Turpeinen, P. Melanen, P. Savolainen, P. Uusi-maa, M. Pessa, Effecs of rapid thermal annealing on strain-compensated GaInNAs/GaAsP quantum well structures and lasers // *Applied Physics Letters*. **78**(1), pp. 91-92 (2001).
22. M. Kondow, T. Kitatani, M.C. Larson, K. Nakahara, K. Uomi, H. Inoue, Gas-source MBE of GaInNAs for long-wavelengtn laser diodes // *Journal of Crystal Growth*, **188**, pp. 255-259 (1998).
23. S. Sato, Y. Osawa, T. Saitoh, I. Fujimura, Room-temperature pulsed operation of 1.3 μm laser diode // *Electron. Lett*, **33**. pp. 386 (1997).